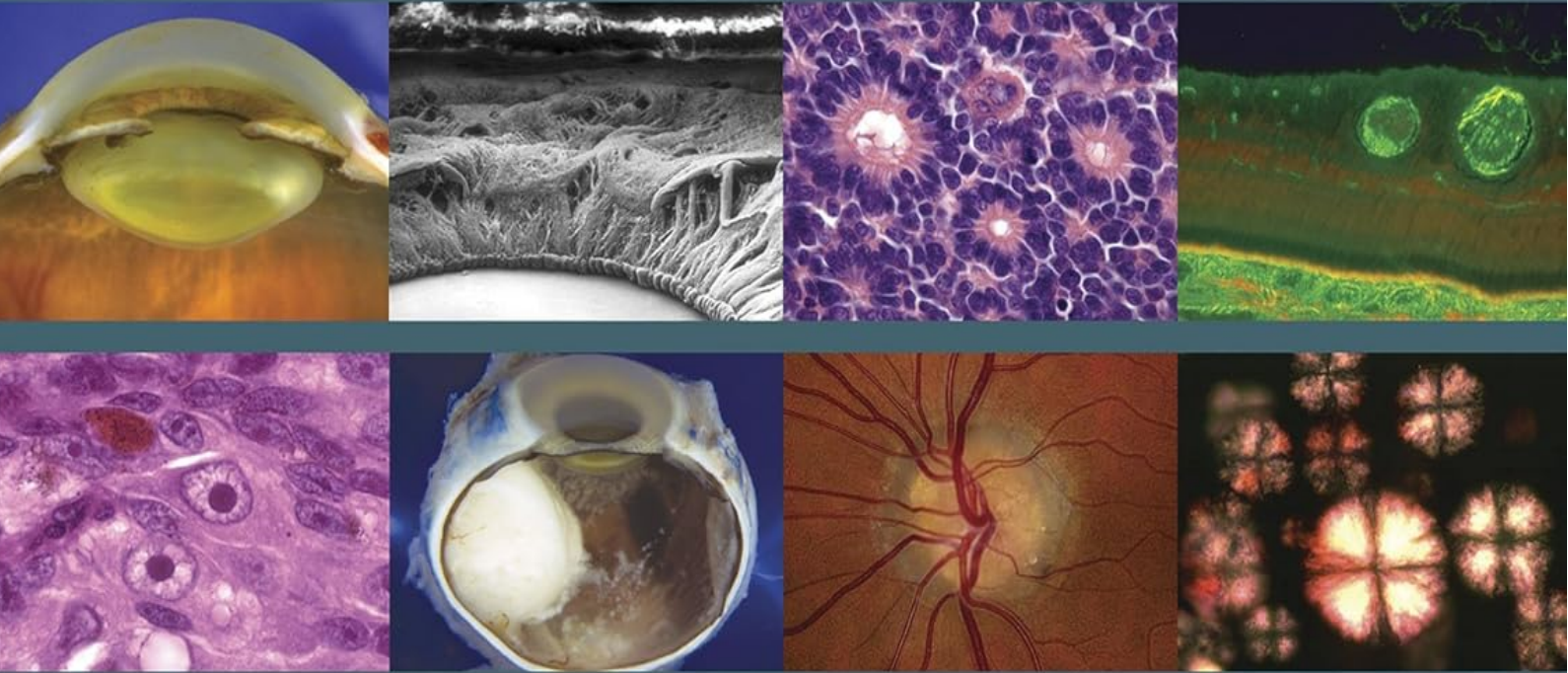




Activate your eBook

Eye Pathology

An Atlas and Text



THIRD EDITION

Ralph C. Eagle, Jr.

 Wolters Kluwer

Eye Pathology

An Atlas and Text

THIRD EDITION

Eye Pathology

An Atlas and Text

THIRD EDITION

Ralph C. Eagle Jr, MD

Director, Department of Pathology
The Noel T. and Sara L. Simmonds Professor of Ophthalmic Pathology
Wills Eye Hospital
Professor of Ophthalmology and Pathology
Sidney Kimmel Medical College of Thomas Jefferson University
Philadelphia, Pennsylvania



Wolters Kluwer

Philadelphia • Baltimore • New York • London
Buenos Aires • Hong Kong • Sydney • Tokyo

Acquisitions Editor: Kel McGowan
Senior Product Development Editor: Emilie Moyer
Senior Production Project Manager: Alicia Jackson
Design Coordinator: Stephen Druding
Manufacturing Coordinator: Beth Welsh
Marketing Manager: Rachel Mante Leung
Prepress Vendor: SPi Global

3rd edition

Copyright © 2017 Wolters Kluwer

Copyright © 2011 by Wolters Kluwer Health / Lippincott Williams & Wilkins.
First Edition copyright © 1999 by W.B. Saunders. All rights reserved. This book is protected by copyright. No part of this book may be reproduced or transmitted in any form or by any means, including as photocopies or scanned-in or other electronic copies, or utilized by any information storage and retrieval system without written permission from the copyright owner, except for brief quotations embodied in critical articles and reviews. Materials appearing in this book prepared by individuals as part of their official duties as U.S. government employees are not covered by the above-mentioned copyright. To request permission, please contact Wolters Kluwer at Two Commerce Square, 2001 Market Street, Philadelphia, PA 19103, via email at permissions@lww.com, or via our website at lww.com (products and services).

9 8 7 6 5 4 3 2 1

Printed in China

Library of Congress Cataloging-in-Publication Data

Names: Eagle, Ralph C., Jr., author.

Title: Eye pathology : an atlas and text / Ralph C. Eagle, Jr.

Description: Third edition. | Philadelphia : Wolters Kluwer, [2017] | Includes bibliographical references and index.

Identifiers: LCCN 2016026753 | ISBN 9781496337177

Subjects: | MESH: Eye Diseases—pathology | Eye—pathology | Atlases

Classification: LCC RE67 | NLM WW 17 | DDC 617.7—dc23 LC record available at <https://lcn.loc.gov/2016026753>

This work is provided “as is,” and the publisher disclaims any and all warranties, express or implied, including any warranties as to accuracy, comprehensiveness, or currency of the content of this work.

This work is no substitute for individual patient assessment based upon healthcare

professionals' examination of each patient and consideration of, among other things, age, weight, gender, current or prior medical conditions, medication history, laboratory data and other factors unique to the patient. The publisher does not provide medical advice or guidance and this work is merely a reference tool. Healthcare professionals, and not the publisher, are solely responsible for the use of this work including all medical judgments and for any resulting diagnosis and treatments.

Given continuous, rapid advances in medical science and health information, independent professional verification of medical diagnoses, indications, appropriate pharmaceutical selections and dosages, and treatment options should be made and healthcare professionals should consult a variety of sources. When prescribing medication, healthcare professionals are advised to consult the product information sheet (the manufacturer's package insert) accompanying each drug to verify, among other things, conditions of use, warnings and side effects and identify any changes in dosage schedule or contraindications, particularly if the medication to be administered is new, infrequently used or has a narrow therapeutic range. To the maximum extent permitted under applicable law, no responsibility is assumed by the publisher for any injury and/or damage to persons or property, as a matter of products liability, negligence law or otherwise, or from any reference to or use by any person of this work.

LWW.com

In Memory of Ewa

This book is also dedicated to my teachers, Myron Yanoff, Ramon L. Font, and Ben S. Fine, and to my former chief, William S. Tasman, for his friendship and strong and unwavering support of ophthalmic pathology during his long and distinguished tenure as ophthalmologist-in-chief at the Wills Eye Hospital.

PREFACE

During the past four decades, I have taught ophthalmic pathology to medical students, interns, and ophthalmologists-in-training at the Wills Eye Hospital, the Lancaster Course in Ophthalmology, and eye hospitals and academic institutions on four continents. I wrote this book because I believed that there was a need for a well-illustrated text that could serve as an introduction to eye pathology. The book has been well received, but a third edition is now necessary because there have been dramatic changes in ophthalmic science and practice since the second edition was submitted for publication in 2010.

In this relatively short time, spectral domain optical coherence tomography has revolutionized the diagnosis and treatment of retinal disorders and is becoming increasingly important in glaucoma and neuro-ophthalmology. SD-OCT has rapidly become the standard of care and continues to increase in quality and resolution. The *in vivo* digital images of ocular anatomy and pathology disclosed by this powerful noninvasive imaging technique are very reminiscent of histologic sections. The accurate interpretation of SD-OCT's striking visual imagery requires a firm foundation in ocular histology and pathology.

Major developments in cornea and external disease have occurred as well. Penetrating keratoplasty is performed less often in this era of resurgent lamellar keratoplasty, and specimens from DALK, DSEK, and refractive surgical procedures present new challenges in interpretation and diagnosis. Specimens from patients with corneal dystrophies are accessioned less often and typically bear the stigmata of prior treatments such as phototherapeutic keratoplasty, which significantly delays surgery in many patients.

Currently, fewer eyes with intraocular tumors are being enucleated as most uveal melanomas undergo eye-sparing radioactive plaque brachytherapy, and an increasing number of infants with retinoblastoma are treated with chemotherapy, delivered intra-arterially or by intravitreal injection. The trend toward evisceration has also decreased the number of blind, painful eyes that are enucleated. Interpretation of the tissue fragments comprising ocular evisceration specimens is often challenging.

Immunohistochemistry is now used routinely to assess and diagnose ocular specimens. In addition, the classification and prognostic assessment of ocular and adnexal neoplasms relies increasingly on powerful molecular genetic tests that profile the expression of tumor genes or detect specific translocations and gene fusion proteins that are diagnostic and prognostic. The genes and molecular mechanisms responsible for an ever-growing number of hereditary ocular disorders continue to be identified, and gene sequencing, which is becoming easier and less expensive to perform, undoubtedly will play a progressively more important role in the tomorrow's medicine.

Ophthalmologists and pathologists need to be familiar with these advances in knowledge and practice that are changing the landscape of ophthalmology and ophthalmic pathology. This text, now in its third edition, has been revised to meet that need.

Written and illustrated solely by the author, *Eye Pathology: An Atlas and Text* serves as a basic introduction to eye pathology that is concise enough to be read and mastered during an ophthalmic pathology rotation. It also is a well-illustrated resource for ophthalmologists-in-training who are studying for board certification in ophthalmology or OKAP examinations. The text should also benefit surgical pathologists who wish to learn more about the pathology of the eye and need a short, well-illustrated reference by the grossing bench or microscope.

The text in the third edition has been updated and lengthened slightly. Some figures have been revised, and new figures and large color photomontages have been added. In addition, 300 new multiple choice questions with explanatory answers have been added to the book's online resources. The online self-assessment quiz section now comprises more than 800 multiple choice questions including 200 based on photos or photomicrographs. The online resources also include a digital version of the book and an image bank.

Why study ophthalmic pathology? Most would agree that a thorough understanding of ocular disease and pathologic mechanisms that cause blindness are prerequisites for quality ophthalmic practice. A physician cannot diagnose a disease that he or she has never heard of. Moreover, ophthalmologists need this knowledge so they can understand, critically assess, or even question the accuracy of diagnoses rendered by pathologists who may have little or no training in ophthalmic pathology.

More than 30 years ago, Dr. Frederick A. Jakobiec eloquently

addressed this question in his introduction to a special issue of the journal *Ophthalmology* dedicated to basic science and ophthalmology. Dr. Jakobiec's* words still ring true today...“Unless one knows the natural course of a disease, it is not possible to decide whether an intervention has been efficacious or not. At a time when we are witnessing the progressive commercialization of ophthalmology and the slackening of traditional standards of professional behavior, one of the few remaining constraints that might prevent us from becoming high-tech mountebanks, peddling star wars’ nostrums that are expensive and potentially meretricious, is our well-founded and ethically enhancing knowledge of ocular disease.”

Ralph C. Eagle Jr,
MD May, 2016

*Jakobiec, FA. Understanding ocular disease: science in the service of ethics (guest editorial), *Ophthalmology*. 1984;91(6):41A–42A.

Contents

Dedication

Preface

Chapter 1. An Introduction to Ocular Anatomy and Histology

Chapter 2. Congenital and Developmental Anomalies

Chapter 3. Inflammation

Chapter 4. Ocular Trauma

Chapter 5. Conjunctiva

Chapter 6. Cornea and Sclera

Chapter 7. The Lens

Chapter 8. Glaucoma

Chapter 9. Retina

Chapter 10. Vitreous

Chapter 11. Intraocular Tumors in Adults

Chapter 12. Retinoblastoma and Simulating Lesions

Chapter 13. Eyelid

Chapter 14. Orbit

Chapter 15. Optic Nerve

Chapter 16. Laboratory Techniques and Special Stains

Index

1 An Introduction to Ocular Anatomy and Histology

A paired, hollow, spherical organ, the human eye is slightly less than an inch in diameter (Fig. 1-1A). Internally, it is divided into anterior and posterior chambers and a much larger vitreous cavity, which comprises most of its posterior segment. The anterior chamber is bounded anteriorly by the cornea and posteriorly by the anterior surfaces of the iris and lens (Fig. 1-1B). The posterior chamber is bounded anteriorly by the iris pigment epithelium (IPE) and laterally by the ciliary processes that form the pars plicata of the ciliary body and posteriorly by the “face” or anterior surface of the vitreous humor. Both anterior and posterior chambers are filled with watery aqueous humor, which is secreted by the ciliary epithelium on the ciliary processes.

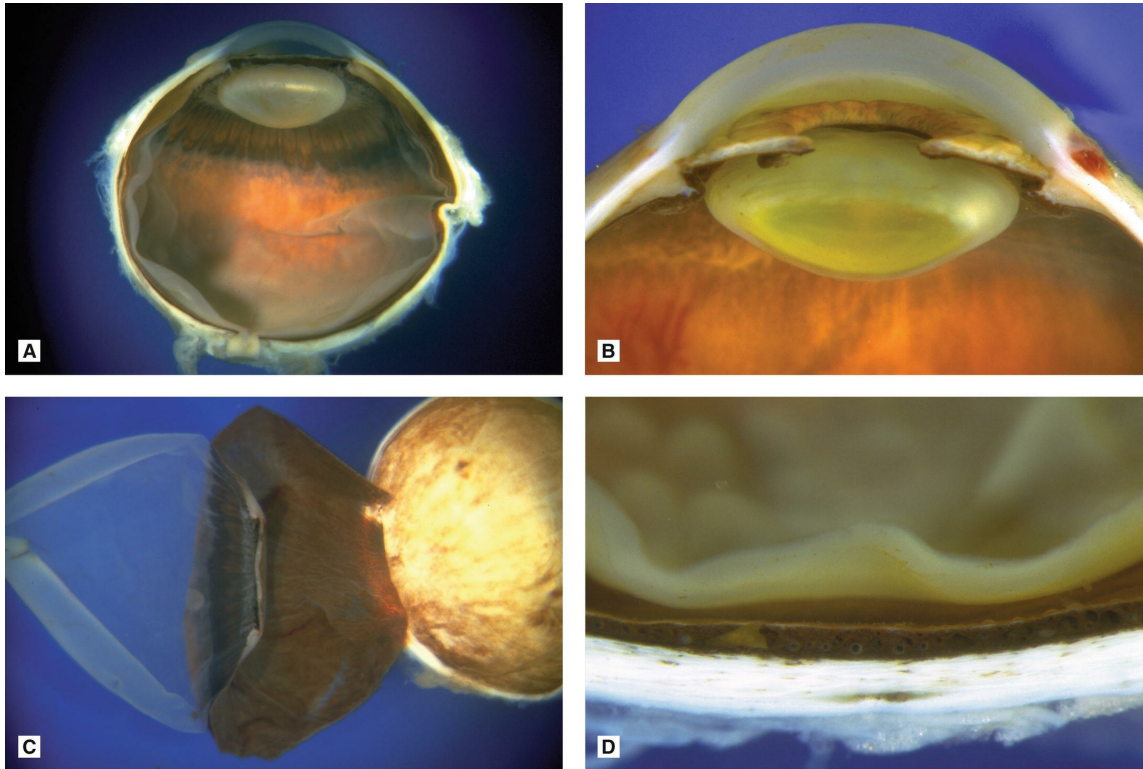


FIG. 1-1. **A.** Slightly less than an inch in diameter, the eye is composed of an anterior chamber and a much larger posterior vitreous cavity. **B.** The anterior chamber is bounded anteriorly by the cornea and posteriorly by the iris and lens. The lens is situated in the posterior chamber behind the pupil. **C.** The eye is composed of three concentric coats that are easily separated during dissection. **D.** Posteriorly, the three coats are evident as the sclera, the pigmented choroid, and the retina.

The vitreous humor fills most of the posterior segment. The most delicate connective tissue in the body, the vitreous humor is a transparent gel composed of hyaluronic acid and a framework of delicate fibrils of type 2 collagen. Centrally, the anterior face of the vitreous abuts the posterior surface of the lens, which is located directly behind the iris in the posterior chamber, and is supported by a suspensory ligament of zonular fibers. The concavity in the anterior face of the vitreous that conforms to the posterior surface of the lens is called the patellar fossa, and the retrolental space of Burger is interposed between the lens and vitreous. Posteriorly, the vitreous lines the inner surface of the retina. Anteriorly, it is firmly adherent to the vitreous base, which straddles the ora serrata, the junction between the peripheral retina and the pars plana of the ciliary body. The vitreous also has relatively firm attachments to the margin of the optic disc and major retinal vessels. A curved channel called the Cloquet canal runs through the center of the vitreous from the lens to the optic nerve.

Overlying the optic nerve head, the posterior part of the Cloquet canal widens to form a space resembling an inverted funnel called the area of Martegiani.

The eye wall is composed of three concentric coats that vary markedly in their cellularity and composition (Fig. 1-1C,D). These three layers are readily separated during gross dissection. The outer coat includes the white sclera, which merges with the transparent cornea at the corneoscleral limbus. Paucicellular and composed largely of dense collagenous connective tissue, the outer layer constitutes the eye's tough fibrous exoskeleton that confines and protects its contents of fluid and delicate neural tissues. The collagenous lamella of the sclera is larger and more irregular than those of the cornea.

The innermost coat of the eye is composed of neuroectodermal tissues derived from the optic cup. Highly cellular and largely devoid of connective tissue, these structures include the neurosensory retina, the retinal pigment epithelium (RPE), the ciliary epithelium, and the IPE. Embryologically, this inner layer of neuroectodermal tissues is derived from an outpouching of the forebrain called the optic vesicle. The neuroectoderm is a polarized layer of epithelial cells with characteristic apical and basal features. Microvilli and cilia typically are found on the apical surface of the cells, which are joined near their apices by intercellular connections called terminal bars. The bases of the cells rest on a basement membrane or basal lamina. The basal lamina serves as the attachment for extracellular matrix material.

The optic vesicle is lined externally by a basement membrane, and the apical surface of its neuroectodermal cells projects into its lumen. Later, as the optic vesicle invaginates to form the optic cup on day 27 of gestation, the apical surfaces of the inner and outer layer of cells become approximated. This "apex-to-apex" orientation continues throughout life. The inner layer of the optic cup goes on to form the posterior layer of IPE, the inner nonpigmented layer of ciliary epithelium, and the neurosensory retina. Its outer layer forms the anterior half of the iris pigment epithelial, which includes the dilator muscle, the outer pigmented layer of ciliary epithelium, and the RPE.

The two layers of cells that comprise the iris and ciliary epithelia retain the "apex-to-apex" orientation found in the optic cup with basal laminae on their external surfaces. Both layers are firmly fused together. Both of the layers are pigmented in the IPE. The ciliary epithelium is a half-pigmented bilayer of cells; its outer layer is pigmented, and its inner layer

is nonpigmented (see [Fig. 1-5D](#)). During microscopy, this “two-toned” bilayer readily serves to identify ciliary body tissue. At the ora serrata, the outer layer of pigmented ciliary epithelium continues posteriorly as the RPE, and the inner layer of nonpigmented ciliary epithelium abruptly thickens to form the neurosensory retina, with its complex lamellar architecture. Posterior to the ora serrata, the layers derived from the inner and outer layers of the optic cup are not fused together as they are in the IPE and ciliary body epithelium. A potential space called the subretinal space is interposed between the retina and the RPE. The apical surfaces of both tissues project into the subretinal space and interdigitate. Retinal detachment or separation is marked by the accumulation of fluid in this potential space.

In routine microscopic sections, the IPE appears to be a single layer, since its dual architecture is largely obscured by intense cytoplasmic pigmentation ([Fig. 1-2D](#)). Both layers are apparent in bleached sections, however. The iris dilator muscle appears as an eosinophilic band on the anterior surface of the IPE. The dilator is not a separate structure. Rather, it is composed of nonpigmented cellular processes with smooth muscle differentiation that arise from the basal surface of the anterior layer of cells. The sphincter muscle of the iris, which encircles and constricts the pupil, is also derived from the IPE, but separates from it during development to form a distinct structure. Continuity of the sphincter muscle with the IPE can be observed microscopically in fetal eyes. The sphincter is about 1 mm in width and is separated from the IPE by a layer of connective tissue that becomes more prominent with increasing age.

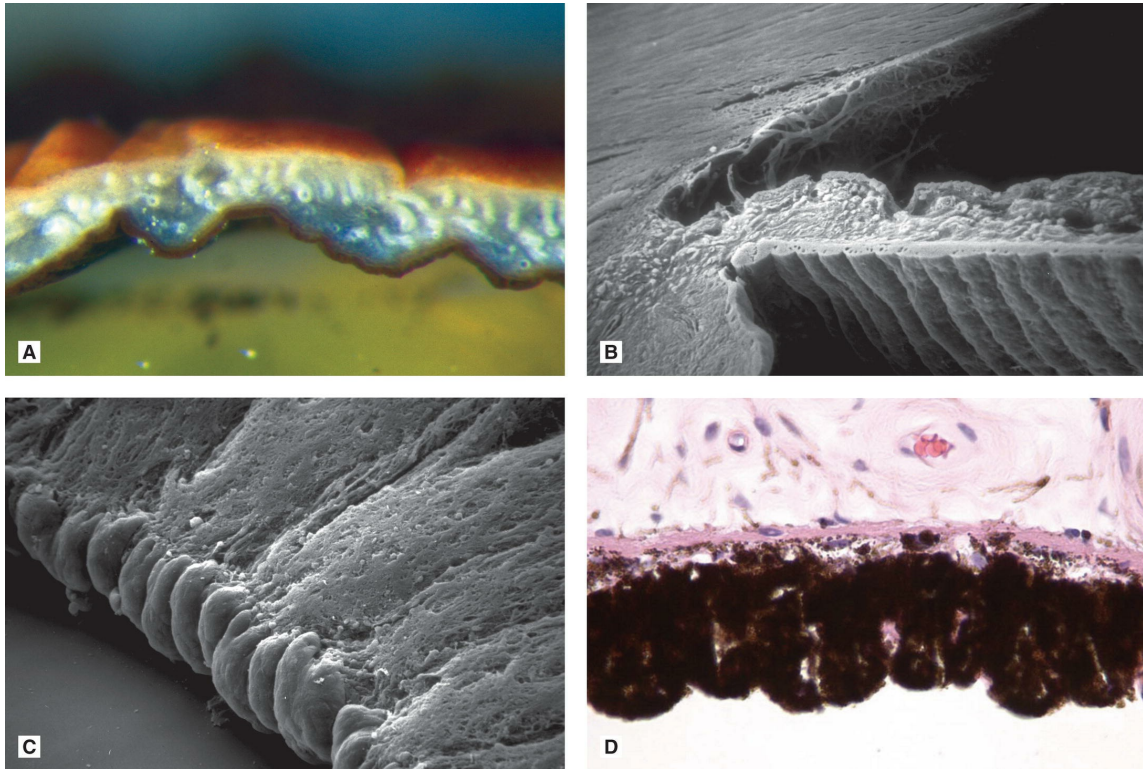


FIG. 1-2. The iris. **A.** The pigment in this brown iris is concentrated in the melanocytes of the anterior border layer. The posterior IPE is maximally pigmented. Cuffs of collagen highlight iris stromal vessels. **B.** SEM shows circumferential ridges on the posterior surface of neuroectodermal IPE. Iris stroma is derived from neural crest. **C.** Termination of IPE at pupillary margin forms beaded pigment ruff. **D.** The two layers comprising the IPE are fused and maximally pigmented. The dilator muscle is evident as an eosinophilic band on its stromal surface. It is composed of cellular processes with smooth muscle differentiation. (**B.** SEM $\times 40$, **C.** SEM $\times 320$, **D.** H&E $\times 250$.)

Clinically, the IPE is visible at the edge of the pupil as the pigment ruff or frill, which corresponds to the margin of the optic cup (Fig. 1-2C). This is the only neuroectodermal tissue of the eye that can be seen with the slit lamp biomicroscope without supplementary lenses. The granules of neuroepithelial melanin in the iris pigment epithelial cells are large and spherical in shape in contrast to retinal pigment epithelial granules, which typically are ellipsoidal. Granules of neuroectodermal melanin are always larger than the dust-like melanosomes found in uveal stromal cells. The IPE is maximally pigmented in all eyes.

A peripheral colony of brain-like tissue, the neurosensory retina is a complex, highly cellular tissue composed of cells that are arranged in regular layers (Fig. 1-3A). Ten retinal layers including the RPE are identified. It is relatively easy to remember the microscopic anatomy of the

retina if one recalls that the retina is a three-neuron system composed of three layers of cells: photoreceptors and first- and second-order neurons. Regarding orientation, the term *inner* refers to retinal layers that are located closest to the vitreous cavity or the center of the eye. *Outer* denotes layers that are located nearer the sclera. The nuclei of retinal cells are arranged in distinct bands called nuclear layers. The nuclei of the photoreceptors and first-order neurons (bipolar cells) form the outer nuclear layer (ONL) and inner nuclear layer (INL), respectively. The retinal ganglion cells (the second-order neurons) comprise the innermost layer of nuclei in the retina. The ganglion cell layer (GCL) varies markedly in thickness. Surrounding the fovea, the GCL is five or more cells thick. Multilamination of the GCL is an excellent histologic marker for the macula or perifoveal part of the retina. The GCL is thin in the peripheral retina. Peripheral to the vascular arcades formed by the superior and inferior temporal retinal arterioles, the ganglion cells form a discontinuous monolayer.

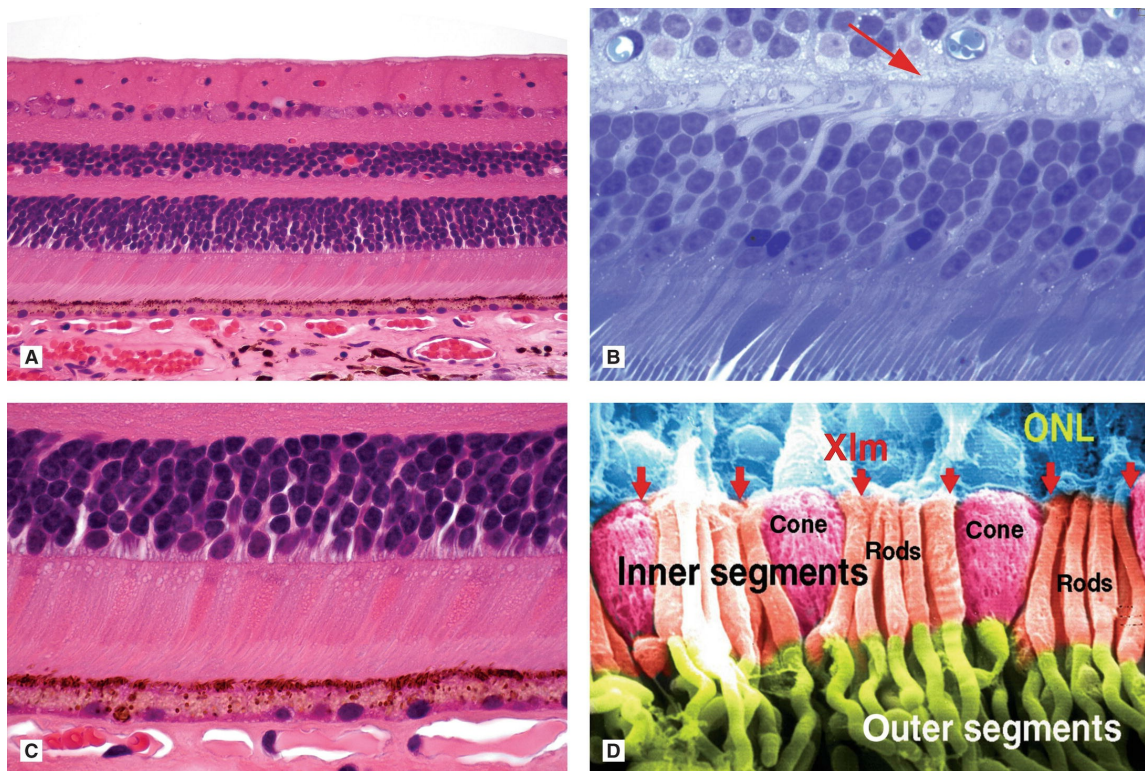


FIG. 1-3. The retina. **A.** The retina is composed of orderly layers of cell nuclei (nuclear layers) and plexiform layers composed of axons and dendrites. The photoreceptors rest on the RPE on the inner surface of the choroid. **B.** The MLM (**top right**) is a linear band of synapses connecting photoreceptor cell axons and bipolar cell dendrites in the anterior part of the OPL. **C.** The inner and outer segments of the photoreceptors project through the fenestrated XLM into the

subretinal space. The tips of the outer segments interdigitate with pigmented processes on the apical surface of the RPE. **D.** False colorized SEM highlights inner and outer segments of rods and cones. Cones are distinguished by the conical configuration of their inner segments. Photoreceptor nuclei comprise ONL. (**A.** H&E $\times 50$, **B.** toluidine blue $\times 250$, H&E $\times 250$, SEM $\times 2,500$.)

The plexiform layers of the retina are composed of axons and dendrites. The outer plexiform layer (OPL) is interposed between the ONL and INL, and the inner plexiform layer separates the INL from the GCL. The inner plexiform layer is truly plexiform: its whole breadth comprises of an intricately interweaving tangle of ramifying neuronal processes. In contrast, only the narrow inner band of the OPL is truly plexiform. Its wider outer part contains an orderly parallel array of photoreceptor axons called Henle fibers. Although Henle fibers occur throughout the retina, the eponym generally is applied to the radially oriented photoreceptor axons that surround the fovea. A line of synaptic connections comprising cone pedicles, rod spherules, and the dendrites of bipolar cells delimits the outer margin of the truly plexiform inner part of the OPL (**Fig. 1-3B**). This linear row of synapses is called the middle limiting membrane (MLM). Like the retina's external limiting membrane (XLM), the MLM is not a basement membrane (the only true basement membrane of the retina is the internal limiting membrane or ILM). The MLM delimits the vascularized inner part of the retina; capillaries from the central retinal artery penetrate no deeper than the MLM. External to the MLM, the retina is avascular and depends on the choroidal circulation for oxygen and nutrients. The OPL is a watershed zone between the dual vascular supplies of the retina. This factor contributes to the localization of edema fluid and hard exudates in OPL.

The INL contains the nuclei of bipolar, amacrine, horizontal, and Müller cells. Bipolar cells predominate. The horizontal cell nuclei are found in the outer, and the amacrine cell nuclei in the inner part of the INL. The nuclei of the Müller cells can lie at any level of the INL. Accessory glial cells including fibrous and protoplasmic astrocytes and oligodendrocyte-like cells are confined to the nerve fiber, ganglion cell, and inner plexiform layers of the retina. Hence, gliosis does not occur after central retinal artery occlusion because these cells are killed.

As we have seen, the orientation of cells in the optic vesicle and optic cup persists in the adult eye. The ILM of the retina corresponds to the basal lamina on the inner layer of the optic cup. A true basement membrane, the ILM is synthesized by the basal foot processes of the giant

glial cells of Müller, which span the entire thickness of the retina. The ILM serves as an attachment point for the fine fibrils of type II collagen that comprise the fibrillar component of the vitreous humor. Intricately, interweaving processes of the Müller cells totally fill the interstices between the retinal neurons and serve to segregate their receptive surfaces. There is little or no extracellular space in the retina.

The Müller cells are polarized. Electron microscopy discloses microvilli on their apical surfaces, which project into the subretinal space between the photoreceptors forming the fiber baskets of Schultze. A belt desmosome of intercellular junctions called the XLM is found in the outer or apical part of the neurosensory retina. Not a true basement membrane, the XLM is composed of permeable adherent junctions (zonulae adherentes) that join the apices of the Müller cells and the rods and cone cells. The XLM is permeable and does not form a barrier to fluid or macromolecules. The inner and outer segments of the rods and cones project through this membrane into the subretinal space where they are surrounded by extracellular matrix material rich in hyaluronidase-resistant acid mucopolysaccharide and interdigitate with cellular processes on the apical surfaces of the RPE cells (Fig. 1-3C). Cone cell nuclei are located next to the XLM in the ONL.

Rods and cones are distinguished light microscopically by the shape of their inner segments (Fig. 1-3D). The inner segments of rods are slender rod-like cylinders, while extrafoveal cones are conical in shape. Highly specialized cones that resemble rods are densely packed in the cone-rich fovea. The inner segments of photoreceptor are divided into two parts: the proximal myoid located nearest to the XLM and more prominent distal ellipsoid (Fig. 1-3C). The myoid contains Golgi apparatus and rough endoplasmic reticulum but few mitochondria. In contrast, the ellipsoid of the inner segments is packed with mitochondria that provide energy for the photochemistry of vision, which occurs in the photoreceptor outer segments. The mitochondria in the ellipsoid are thought to be responsible for the second of the four hyperreflective bands in the outer retina revealed by spectral domain ocular coherence tomography (SD-OCT) that serves as a clinical marker for healthy photoreceptors.

The inner and outer segments of the photoreceptors are joined by a connecting cilium that has the characteristic 9 + 0 pattern of microtubular doublets found in central nervous system cilia. Photoreceptors probably are derived from modified cilia, which are found on the apical surface of cells. Several inherited retinal disorders are caused by mutations in genes

coding constituents of cilia.

The outer segments of the photoreceptor contain thin discs composed of cellular membranes that are arranged in stacks. The arrangement of the membranous discs has been likened to a stack of coins or potato chips packaged in cylindrical containers. Visual pigments including rhodopsin are incorporated as transmembrane proteins in the disc membranes. Separate, free-floating discs occur in rods. The discs in cone outer segments are not separate structures; they comprise a continuous, sinuously folded structure formed by invaginations of the outer cell membrane.

Photoreceptor outer segments project from the apical surface of the retina into the subretinal space where they are enveloped by microvillous processes on the apical surface of the RPE, the polarized monolayer of pigmented cells derived from the outer layer of the optic cup. The RPE cells are firmly joined near their apices by a girdle of intercellular connections called *zonulae occludentes*. These tight junctions form a barrier to the passage of molecules and constitute the outer part of the blood–retinal barrier. Large ellipsoidal granules of melanin pigment measuring $\sim 1 \mu$ in diameter are found in the apical cytoplasm of the RPE cells. Granules of lipofuscin pigment fill the basal cytoplasm. The latter “wear-and-tear” pigment is derived from the incomplete digestion of photoreceptor outer segments by the RPE’s phagolysosomal system and gradually accumulates with age. The lipofuscin is relatively inapparent in routine hematoxylin and eosin (H&E) sections, but the pigment is autofluorescent and is vividly disclosed by UV fluorescent microscopy (Fig. 1-4D). The nuclei of the RPE cells are located in the basal cytoplasm near Bruch membrane.

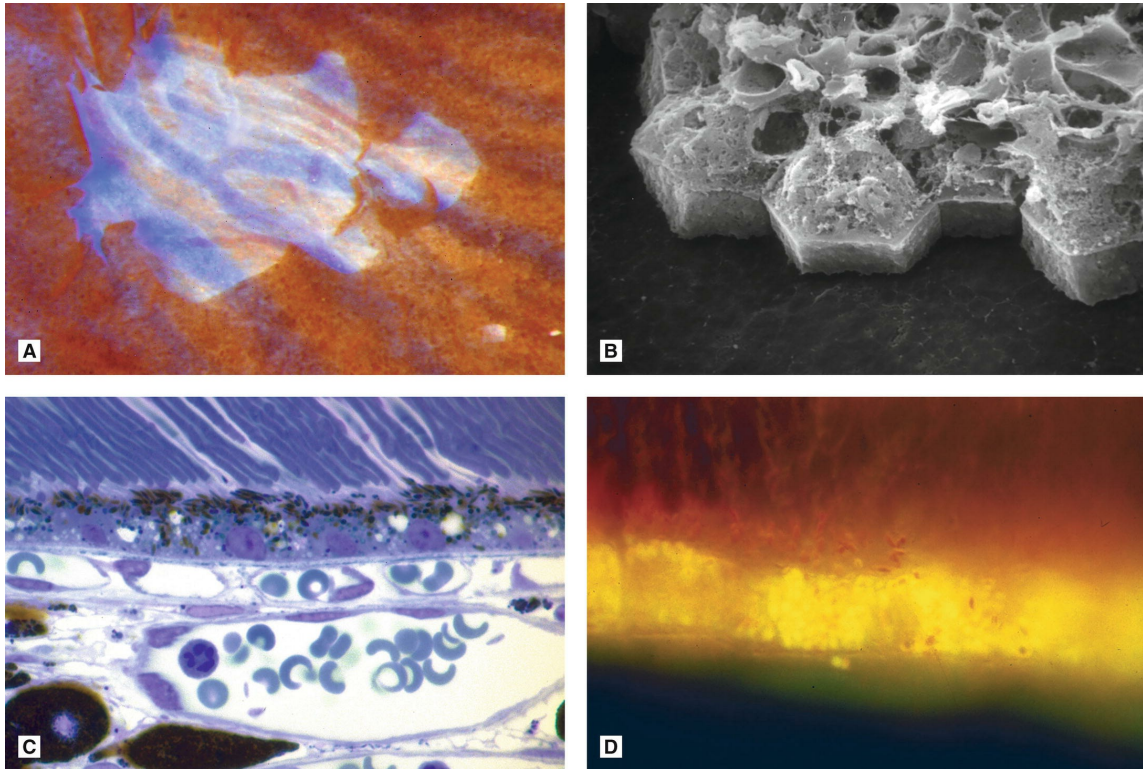


FIG. 1-4. The retinal pigment epithelium (RPE). **A.** The RPE is largely responsible for the color of the fundus. Rip in pigmented layer discloses large vessels in underlying choroid separated by uveal pigment. **B.** SEM shows hexagonal monolayer of RPE cells covering inner surface of the Bruch membrane. **C.** Photomicrograph shows elliptical granules of RPE melanin in apical cytoplasm of RPE cells. The choriocapillaris abut the outer surface of the Bruch membrane. **D.** Fluorescent microscopy (**bottom right**) discloses *yellow* granules of autofluorescent lipofuscin pigment in the basal cytoplasm of the RPE cells. (**B.** SEM $\times 1,250$, **C.** toluidine blue $\times 250$, UV fluorescent microscopy $\times 400$.)

An intact layer of RPE is vital to the health and function of the adjacent neurosensory retina (Fig. 1-4). In flat preparations, the cells comprising this pigmented monolayer are hexagonal in shape, resembling the familiar pattern of bathroom tile (Fig. 1-4B). The pigment in the RPE is largely responsible for the reddish-brown color of the fundus seen grossly or ophthalmoscopically (Fig. 1-4A). This is readily demonstrated in the laboratory by focally denuding the Bruch membrane with a cotton swab. Removal of the RPE discloses the larger choroidal vessels, which are visible through the Bruch membrane, which is semitransparent. Melanin pigment within choroidal melanocytes between the vessels serves to highlight the latter. In heavily pigmented people, the density of pigmentation between the vessels may impart a tigroid or tiger-striped

appearance to the fundus.

The RPE rests on a specialized layer of connective tissue called the Bruch membrane, which rests on, and delimits the inner surface of the choroid (Fig. 1-4C). The Bruch membrane is a sandwich-like structure composed of extracellular matrix material. Its inner and outermost layers are the basement membranes of the RPE cells and the endothelial cells of the choriocapillaris, respectively. The basement membrane of the RPE corresponds to the basement membrane on the outer surface of the optic cup. The Bruch membrane is largely composed of type 1 collagen and has a central core of elastic tissue. As we age, the Bruch membrane gradually thickens and becomes increasingly periodic acid–Schiff (PAS) positive. Basophilic foci of calcification are often found in the posterior parts of the Bruch membrane in the elderly. Transmission electron microscopy demonstrates that the thickening of the Bruch membrane is caused by the gradual accumulation of linear and vesicular structures.

The choroid is the posterior and largest part of the uveal tract, the eye's central coat, which is interposed between the outer sclera and the innermost layer of neuroectodermal tissue (Fig. 1-1D). Intermediate in cellularity, the uveal tract is pigmented and richly vascular. The term uveal reflects the fanciful resemblance of this coat to a black-purple grape (uva = grape in Latin) noted when early anatomists removed the sclera. Derived from neural crest, the uvea comprises the iris stroma, the stroma of the ciliary body, and the choroid.

The highly vascular choroid contains three layers of blood vessels that increase in size as they near the sclera (Fig. 1-3A). An interconnected layer of leaky, fenestrated capillaries called the choriocapillaris rests directly beneath the Bruch membrane (Fig. 1-3A,C). A second layer of medium-size vessels called the Sattler layer and an outer layer of larger vessels called the Haller layer also are present. The choroidal stroma contains connective tissue and dendritic melanocytes that vary in their pigment content depending on the patient's race and eye color. An equivalent number of melanocytes is present in all races, but darkly pigmented individuals have larger cells filled with larger melanin granules. The melanin granules found in uveal melanocytes are quite small and dust like. They are readily distinguished from the large ellipsoidal granules of melanin found in the apical cytoplasm of the RPE cells.

The middle part of the uveal tract called the ciliary body is interposed between the iris and the choroid (Fig. 1-5). The ciliary body has two major components, the pars plicata (also called the “corona ciliaris”) and the pars

plana (Fig. 1-5B). The anterior pars plicata is composed of a ring of 70 to 80 ciliary processes. The ciliary processes project into and encircle the posterior chamber, and their nonpigmented epithelial cells secrete the watery aqueous humor that fills that cavity and the anterior chamber. The aqueous humor flows through the pupil toward specialized “drains” located in the anterior chamber “angle” formed by the junction of the iris and cornea. Small white nodules occasionally are observed incidentally on individual ciliary processes during gross dissection, particularly in the eyes of older individuals. These represent small foci of pseudoadenomatous proliferation of the nonpigmented ciliary epithelium called Fuchs (or coronal) adenomas. They undoubtedly represent the smallest eponymic “neoplasms” in the human body.

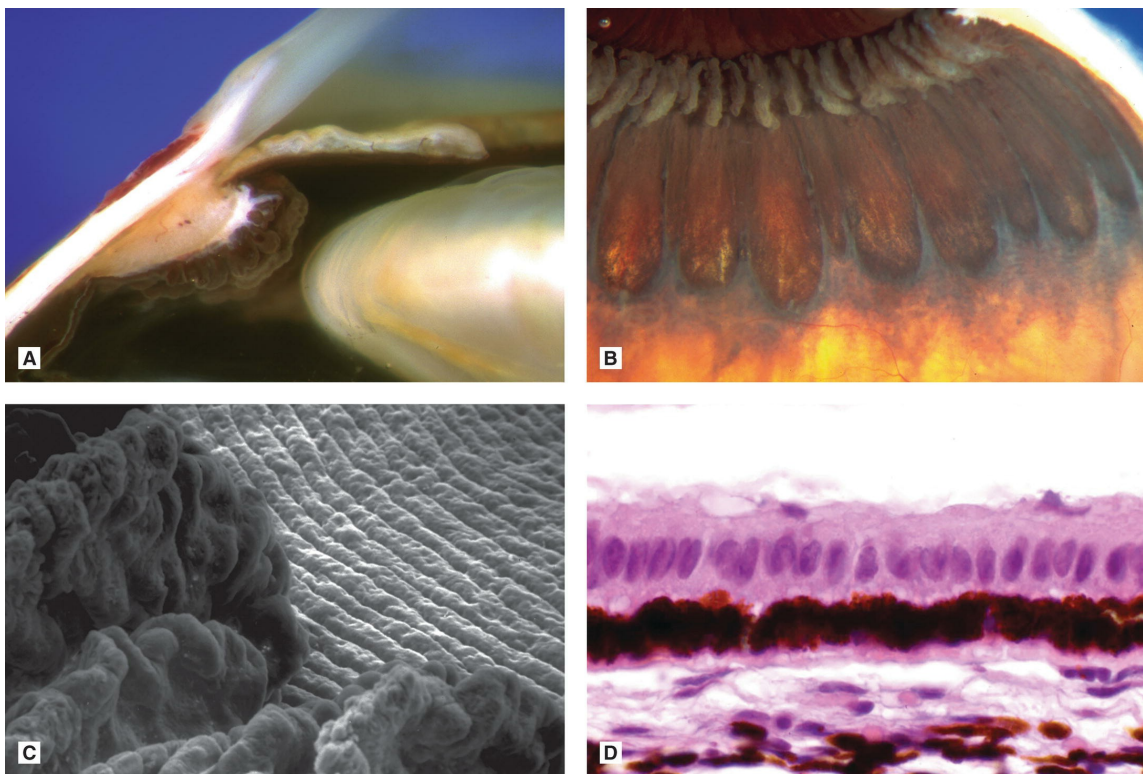


FIG. 1-5. Ciliary body. **A.** The pars plicata of the ciliary body is composed of ciliary processes, which project into the posterior chamber directly behind the iris. **B.** The flat pars plana is interposed between the ring of ciliary processes comprising the pars plicata and the retina. The ora serrata is the junction between the pars plana and the retina. The nasal ora serrata, shown here, has prominent dentate processes and concave oral bays. **C.** Scanning electron micrograph shows convoluted surface of ciliary processes and circumferential folds on the posterior surface of IPE. **D.** The ciliary epithelium, shown here on the pars plana, is a half-pigmented bilayer. Its nonpigmented inner layer is continuous with the retina at the ora serrata. (C. SEM $\times 50$, D. H&E $\times 250$.)

The ciliary processes of infants are smooth and pigmented. With age, the processes become increasingly thickened, convoluted, and hyalinized as collagenous connective tissue accumulates around the vessels in their cores (Fig. 1-5C,D). The hyalinized ciliary processes in older patients appear white. With experience, one can roughly estimate a patient's age from the degree of hyalinization evident grossly or microscopically. The pars plana or flat part of the ciliary body is located posterior to the pars plicata and forms a circular band that extends to the ora serrata. The term ora serrata, which means "toothed mouth," is derived from the serrated appearance of this junction caused by the presence of anteriorly projecting dentate processes of peripheral retina separated by concavities called oral bays (Fig. 1-5B). Dentate processes and oral bays are prominent in the nasal ora serrata, while the temporal ora is relatively smooth. This finding can serve as anatomic landmark to orient the eye during gross examination. In some eyes, elongated dentate processes of peripheral retinal tissue called meridional complexes deeply invade, or even bridge, the pars plana. Posterior to the ora, the peripheral retina often has a moth-eaten pattern of darker spaces reflecting the almost ubiquitous presence of peripheral microcystoid degeneration (see Chapter 9).

The bilayer of half-pigmented ciliary epithelium that forms part of the eye's inner neuroectodermal layer (Fig. 1-5D) is discussed above. The stroma of the ciliary body is composed largely of smooth muscle. In routine histologic sections, the ciliary muscle appears as an elongated triangle, but in actuality, the structure is a circular sphincter. The ciliary muscle has longitudinal, radial, and circular parts. The longitudinal ciliary muscle of Brücke attaches to the sclera spur, a ridge of connective tissue that is located directly behind the trabecular meshwork and the canal of Schlemm. The scleral spur is the only spot where the ciliary body is firmly attached to the sclera. The ciliary muscle's primary function is focusing or accommodation, which is discussed in the lens section below.

The iris is the anterior, visible part of the uveal tract (Fig. 1-2). The structure is named after Iris, the Greek goddess of the rainbow, an appellation that undoubtedly reflects the range of eye colors found in different peoples. The iris has two components, the posterior IPE derived from neuroectoderm (see above) and the iris stroma, derived from neural crest. Its major component, the iris stroma, is a loosely arranged tissue that contains pigmented and nonpigmented cells set in an abundant extracellular matrix containing bundles of type I collagen fibrils and hyaluronidase-sensitive glycosaminoglycans. The cells include

melanocytes and fibroblasts. The greatest concentration of iris melanocytes is found in the avascular anterior border layer deep to an inconspicuous discontinuous sheet of fibroblasts (Fig. 1-2A). The iris vessels have an undulating radial orientation. Ensheathed by a thick mantle of collagen fibers, these “thick-walled” vessels have a characteristic histologic appearance that is not encountered elsewhere in the body. The characteristic histologic appearance of its vessels serves to distinguish iris from choroidal tissue in evisceration specimens. Most iris vessels are located in the middle layers of the iris stroma. In blue irides, radiating iris vessels are visible clinically because the melanocytes comprising the anterior border layer lack pigment and are transparent. The melanocytes in darker irides are opacified by pigment, obscuring the vessels. In general, the number and size of melanin granules within iris melanocytes increases in darker irides.

The anterior surface of the iris has an irregular contour. The pupillary portion of the iris, which is located central to the roughly stellate collarette is thinner. Embryologically, this thinning results from atrophy of the anterior stroma caused by resorption of the pupillary membrane. The anterior surface of broader, thicker peripheral ciliary zone is grooved by contraction furrows. Defects in the anterior stroma called the crypts of Fuchs are evident clinically. The iris muscles are discussed above. Heavily pigmented, rounded clump cells of Koganei are often found in the stroma near the sphincter muscle. These can be melanophages (type 1) or displaced neuroepithelial (type 2) cells.

The crystalline lens is situated in the posterior chamber behind the iris (Fig. 1-6). The lens is the only large transparent cellular tissue in the body and is the only intraocular structure that is derived embryologically from the surface ectoderm. Early in gestation, the surface ectoderm overlying the optic vesicle thickens to form the lens placode, which subsequently invaginates to form the lens vesicle, as the neuroectodermal optic vesicle invaginates to form the optic cup. The epithelial cells of the posterior part of the vesicle elongate anteriorly forming the primary lens fibers that fill the cavity of the optic vesicle. These fibers persist as the central embryonic nucleus in the adult lens. The anterior layer of cells persists as the anterior lens epithelium throughout life (Fig. 1-6B). Secondary lens fibers are formed by division of lens epithelial cells near the equator of the lens. Seven to eight millimeters in length, these long, strap-like cells extend from the anterior to the posterior pole of the lens, totally enveloping the nucleus. The formation of secondary lens fibers continues throughout life;

new fibers are laid down peripherally as concentric lamellae in an onion-like fashion. The nuclei of the newly formed peripheral lens fibers form a curved bow near the equator (Fig. 1-6C). These highly specialized epithelial cells lose their nuclei shortly after formation. Tightly packed in a nearly paracrystalline fashion (Fig. 1-6D), the lens fibers are joined together by ball-and-socket joints that minimize extracellular space. The lens has no vessels or nerves and is almost totally devoid of connective tissue, except for its thick enveloping capsule of basement membrane (Fig. 1-6B). The anterior capsule is much thicker than the posterior capsule, whose caliber is less than the diameter of an erythrocyte. Like other basement membranes, the lens capsule stains intensely with the PAS stain. The lens epithelial cells retain the ability to synthesize collagen and may do so under pathologic conditions.

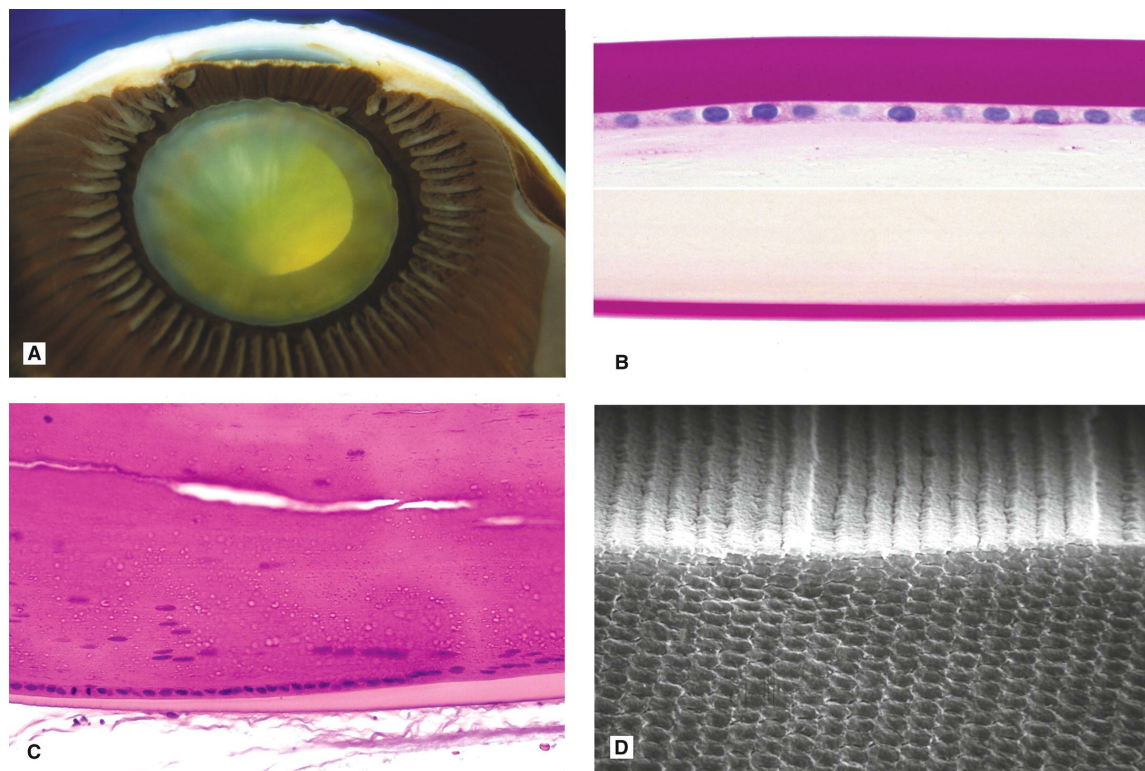


FIG. 1-6. The lens. **A.** The lens is situated in the posterior chamber behind the iris. The lens is composed of highly differentiated epithelial cells called lens fibers. **B.** A monolayer of cuboidal lens epithelial cells is present beneath the anterior lens capsule. The posterior capsule is much thinner. **C.** The epithelial monolayer terminates at the equatorial lens bow, where the cells elongate to form the secondary lens fibers. **D.** SEM shows that the lens fibers are tightly packed in a paracrystalline fashion. (**B.** H&E $\times 100$, **B.** top and bottom, PAS $\times 250$, **D.** SEM $\times 160$.)

The primary optical function of the lens is focusing or accommodation. Divergent light rays from near objects must be bent or refracted more to sharply focus them on the retina. When a near object (e.g., this page) is examined, the ciliary muscle contracts, relaxing the tension on the zonular fibers that form the suspensory ligament of the lens (Fig. 1-7). The ciliary muscle is a circular or sphincter muscle. Its central aperture becomes smaller when it contracts. When distant objects are examined and the eye is at rest, the zonular fibers pull on the lens and flatten it. Relaxation of the zonular fibers during accommodation allows the lens to assume a more spherical configuration, which has a shorter radius of curvature and greater refractive power. Refractive power is inversely proportional to the radius of curvature of a lens.

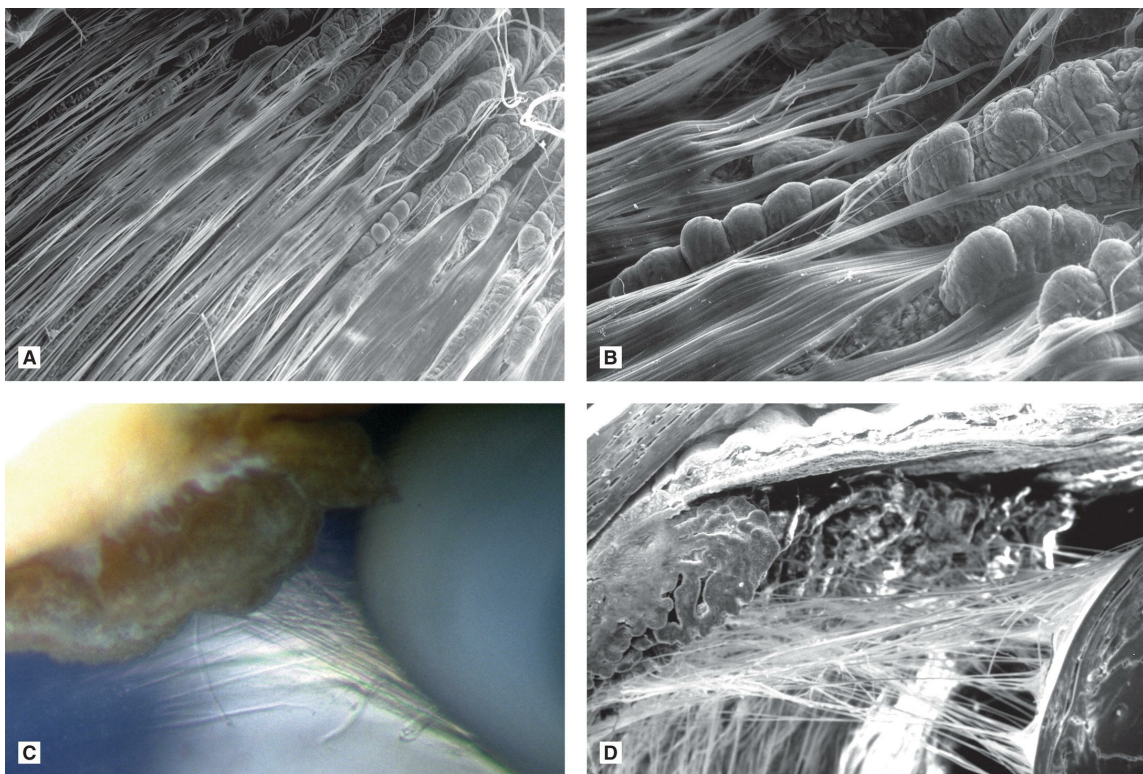


FIG. 1-7. The suspensory ligament of the lens. **A.** SEM discloses zonular fibers traversing the pars plana. **B.** Bundles of zonular fibers pass through valleys between ciliary processes. **C.** Two groups of zonular fibers are disclosed by retroillumination in macrophoto. **D.** Anterior and posterior groups of zonular fibers delimit the triangular canal of Hanover at the lens equator. (**A.** SEM $\times 10$, **B.** SEM $\times 80$, **D.** SEM $\times 20$.)

The cornea (Fig. 1-8) is the eye's major refractive element with an optical power of ~ 45 diopters. It is the anterior, transparent part of the eye's tough outer fibrous coat and is continuous with the sclera at the limbus. The bulk

of the cornea is composed of interweaving lamellae of type I collagen fibers, which are spaced in an exquisitely regular fashion. Artifactitious clefts separate the stromal lamella in routine histologic sections (Fig. 1-8A). The stroma contains flattened dendritiform fibroblast-like cells called keratocytes. A nonkeratinized epithelium five cells in thickness covers the anterior surface of the cornea (Fig. 1-8B). This is composed of basal cells, wing cells, and flattened surface squamous cells. The epithelium normally has an inconspicuous basement membrane and rests on a feltwork of modified stroma called the Bowman membrane or layer, which appears as a homogeneous, hyaline band. A delicate monolayer of flattened endothelial cells, derived embryologically from the neural crest, lines the posterior surface of the cornea (Fig. 1-8C,D). The endothelium secretes a thick basement membrane called the Descemet membrane, which stains intensely with the PAS stain (Fig. 1-8C). Anvil-shaped, hyaline excrescences called Hassall-Henle warts stud the inner surface of the peripheral part of Descemet membrane in older patients. They resemble the guttae that occur in the central cornea in Fuchs endothelial dystrophy.

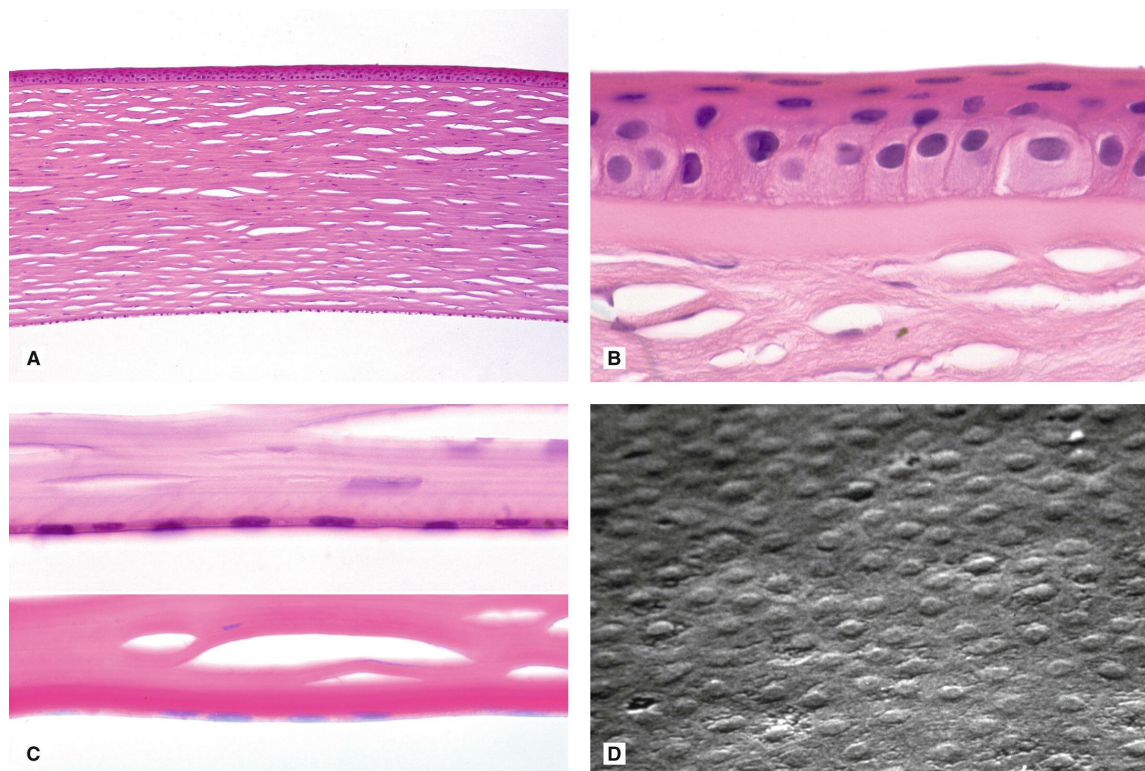


FIG. 1-8. The cornea. **A.** Most of the cornea is composed of collagenous stroma with keratocytes and lamellae separated by artifactitious clefts. **B.** The corneal epithelium rests on the anterior surface of the Bowman layer, a hyaline band of modified stroma. The epithelium is typically five cells in thickness. **C.** A flattened monolayer of corneal endothelial cells rests on the posterior surface of

the Descemet membrane, which is PAS positive (**below**). **D.** SEM discloses a regular mosaic of endothelial cells. (**A.** H&E $\times 50$, **B.** H&E $\times 250$, **C. top**, H&E $\times 250$, **bottom**, PAS $\times 250$, **D.** SEM $\times 160$.)

The intraocular pressure is governed by a delicate balance between the production of aqueous humor by the nonpigmented ciliary epithelial cells and its egress or outflow from the eye. Most aqueous humor exits via the traditional aqueous outflow pathway that consists of the trabecular meshwork and the canal of Schlemm, which are located in the peripheral anterior chamber in the anterior or corneoscleral part of the angle formed by the cornea and peripheral iris (**Fig. 1-9**). Smaller amounts of aqueous exit through nontraditional pathways that include iris vessels and posterior uveoscleral outflow via the ciliary body and the vortex veins.

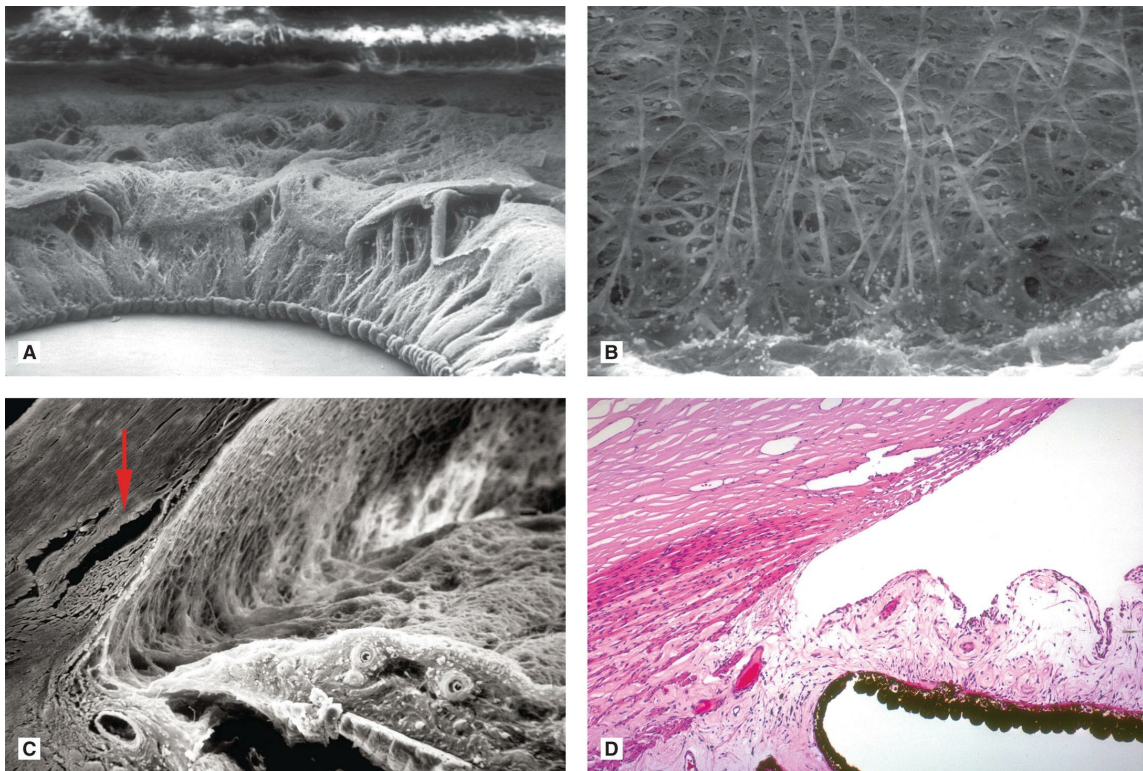


FIG. 1-9. The iridocorneal angle and aqueous outflow pathways. **A.** Electronic charging artifact highlights the trabecular meshwork in the periphery of the anterior chamber in this SEM. **B.** Thin trabecular beams comprising inner part of trabecular meshwork are evident in SEM. **C.** Arrow in SEM points to the canal of Schlemm in the outer wall of the iridocorneal angle external to the trabecular meshwork. **D.** The trabecular meshwork and canal of Schlemm are nestled in the anterior crotch of the scleral spur. The longitudinal ciliary muscle inserts onto the posterior aspect of the spur. (**A.** SEM $\times 20$, **B.** SEM $\times 80$, **C.** SEM $\times 60$, **D.** H&E $\times 50$.)

The trabecular meshwork is a sieve-like structure that is nestled in the anterior crotch of the scleral spur (Fig. 1-9B–D). The scleral spur serves as an important anatomic landmark in both clinical and pathologic practice. The longitudinal fibers of the ciliary muscle are firmly attached to the posterior aspect of the scleral spur (Fig. 1-9D). During microscopy, the spur is found by following the ciliary muscle fibers to their insertion. The trabecular meshwork is composed of an interconnected network of small beams or trabeculae (Fig. 1-9B). The beams are made of collagen with a central core of elastic tissue and are encompassed by trabecular endothelial cells and a thin layer of endothelial basement membrane. The inner, corneoscleral part of the meshwork is composed of concentrically oriented plates of connective tissue containing pores, which are out of register. The interstices of the meshwork do not communicate directly with the lumen of the canal of Schlemm, but are separated from it by a thin layer of extracellular matrix material called the juxtacanalicular connective tissue. Schlemm canal is a modified vein that is lined by a continuous layer of endothelial cells. Schlemm canal runs circumferentially around the chamber angle, giving off branches or collector channels that traverse the sclera and discharge their contents into the epibulbar veins via the aqueous veins of Ascher.

The anterior surface of the eyeball and the posterior surface of eyelids are covered by a delicate transparent mucous membrane called the conjunctiva. The term conjunctiva is derived from Latin meaning “to bind together.” It connects the eye with the eyelids.

The conjunctiva consists of a nonkeratinized stratified columnar epithelium that rests on a connective tissue stroma or substantia propria (see Fig. 5-1). The conjunctival epithelium is two to five cells in thickness and contains mucous glands called goblet cells whose contents appear clear or bluish in routine H&E sections and are vividly PAS positive. Goblet cells are more numerous nasally, especially in the semilunar fold (plica semilunaris).

Topographically, the conjunctiva is divided into bulbar, forniceal, and tarsal (or palpebral) parts. The bulbar conjunctiva covers the anterior surface of the eyeball and is freely movable. The stroma or substantia propria of the bulbar conjunctiva is composed of loose, areolar connective tissue and is easily ballooned-up by edema fluid (chemosis) or injected anesthetic. In contrast, the palpebral conjunctiva is firmly adherent to the tarsal plate and does not move freely. Multiple epithelial invaginations or crypts called the pseudoglands of Henle usually occur in the palpebral

conjunctiva. The forniceal conjunctiva that arches around the superior and inferior cul-de-sacs is redundant and folded to facilitate eye movements. Several small accessory lacrimal glands of Krause are found beneath the forniceal conjunctiva, and accessory glands of Wolfring occur at the upper and lower margins of the tarsal plates. Lymphocytes and plasma cells normally are found in the conjunctival stroma and constitute part of the eye's normal defense mechanisms.

The caruncle is a small fleshy nodule located on the nasal surface of the eye medial to the semilunar fold. The term caruncle means "a little piece of flesh." An island of skin surrounded by conjunctiva, the caruncle is covered by keratinized squamous epithelium with fine vellus hairs. In addition to pilosebaceous units, the stroma contains fat and lobules of accessory lacrimal gland tissue (the glands of Popoff).

The eyelids are flaps of modified skin with highly modified epidermal appendages that cover and protect the eye (Fig. 13-1A–F). The anterior surface of the eyelid is covered by skin, and its posterior surface is lined by a mucous membrane, the palpebral conjunctiva, which is closely applied to the tarsal plate. The tarsal plate is a curved plate of dense connective tissue that serves as the lid's internal skeleton. Striated fibers of the orbicularis muscle are found between the skin and the anterior surface of the tarsus. The orbicularis muscle encircles the eyelid fissure forming a large sphincter that functions during eyelid closure. The bundles of the orbicularis are sectioned transversely in standard histologic sections. A mucocutaneous junction between eyelid skin and conjunctiva occurs near the eyelid margin. Here, the epidermis is mildly thickened and has small rete ridges. Just anterior to the lid margin, slit lamp biomicroscopy discloses a line of tiny meibomian gland orifices. The meibomian glands are large sebaceous glands that occupy almost the entire length of the tarsal plate and are oriented perpendicular to the lid margin. The oily secretion of the meibomian glands helps to retard evaporation of the tear film. About 25 meibomian glands are present in the upper lid and 20 in the lower lid. The meibomian glands in the upper lid are much longer, reflecting the greater length of the upper tarsal plate (11 mm). The upper lid is identified grossly and in tissue sections by the length of the tarsal plate and the lid's roughly rectangular shape. The shape of the lower lid is roughly triangular. The greater mass of meibomian gland tissue in the upper tarsus probably explains why sebaceous carcinoma occurs most often in the upper lid. The eyelid fissure is encircled by a protective ring of cilia (eyelashes). The hair bulbs of the cilia are located deep within the lid

next to the tarsal plate. Malignant tumors such as sebaceous gland carcinoma that arise deep in the substance of the lid often produce loss of lashes (madarosis).

Other eyelid glands bear eponyms. The sebaceous glands that accompany the eyelashes are the glands of Zeis. Sebaceous glands are holocrine glands. The glandular secretion called sebum is composed of entire cells (*holos*—whole). Cellular division occurs in the peripheral germinative layer of sebaceous gland lobules. As new cells form, the older cells are pushed toward the center of the glandular lobule. The cells degenerate as they mature. Their nuclei become karyorrhectic and pyknotic, and the cytoplasm becomes intensely lipidized and foamy.

The glands of Moll are apocrine sweat glands. Their dilated lumina are lined by tall, eosinophilic cells capped with the “apical snouts” that characterize apocrine decapitation secretion. Eccrine sweat glands, which bear no eponym, also are found. Glandular epithelial cells remain intact during eccrine secretion. The glands of Wolfring or Ciaccio are small accessory lacrimal glands that are located at the proximal margins of the tarsal plates. There are two to five glands of Wolfring at the upper margin of the superior tarsal plate and two glands at the lower margin of the lower tarsus. Other accessory lacrimal glands called the glands of Krause are found near the conjunctival fornix. The accessory lacrimal glands are responsible for baseline tear secretion. The main lacrimal gland releases copious amounts of watery secretion (endogenous irrigating fluid) in response to emotional stimuli or severe ocular irritation.

The eye is contained in a protective pear-shaped cavity in the skull called the orbit, which contains about 30 mL of highly specialized tissue (see [Fig. 14-1](#)). Other orbital contents include the optic nerve, which is a specialized tract of the central nervous system; the cartilaginous trochlea, smooth and striated muscle; vessels; nerves; fatty and fibrous connective tissue; and the lacrimal gland, a minor salivary gland. The orbit communicates with the intracranial cavity through several fissures and foramina, and several of its bony walls contain paranasal sinuses. The eye and the remainder of the orbital contents, which are delimited anteriorly by a septum of fibrous tissue, are protected by the eyelids, retractable flaps of skin equipped with highly specialized epidermal appendages. The epithelial-lined components of the nasolacrimal drainage system are located in the inferonasal part of the orbit.

The optic nerve is a tract of the central nervous system that connects the eye and the brain ([Fig. 1-10](#)). The nerve has intraorbital,

intraocular, and intracranial portions and is about 50 mm in total length. It is composed of the axons of the retinal ganglion cells; interstitial cells including oligodendrocytes, astrocytes, and microglia; and fibrovascular septa of the pia mater. The retinal nerve fibers exit the eye through the lamina cribrosa in the posterior sclera and extend to the optic chiasm and then to the lateral geniculate body via the optic tracts. Behind the lamina cribrosa, the axons are myelinated. Here, the nerve measures about 3 mm in diameter. In contrast, the diameter of the optic disc is only 1.5 mm. Dense collagenous dura, the spidery trabeculated arachnoid and the vascularized pia mater comprise the meninges of the optic nerve. The optic nerve is encompassed by firmly adherent pia mater, and its substance is compartmentalized by septa of pial connective tissue.

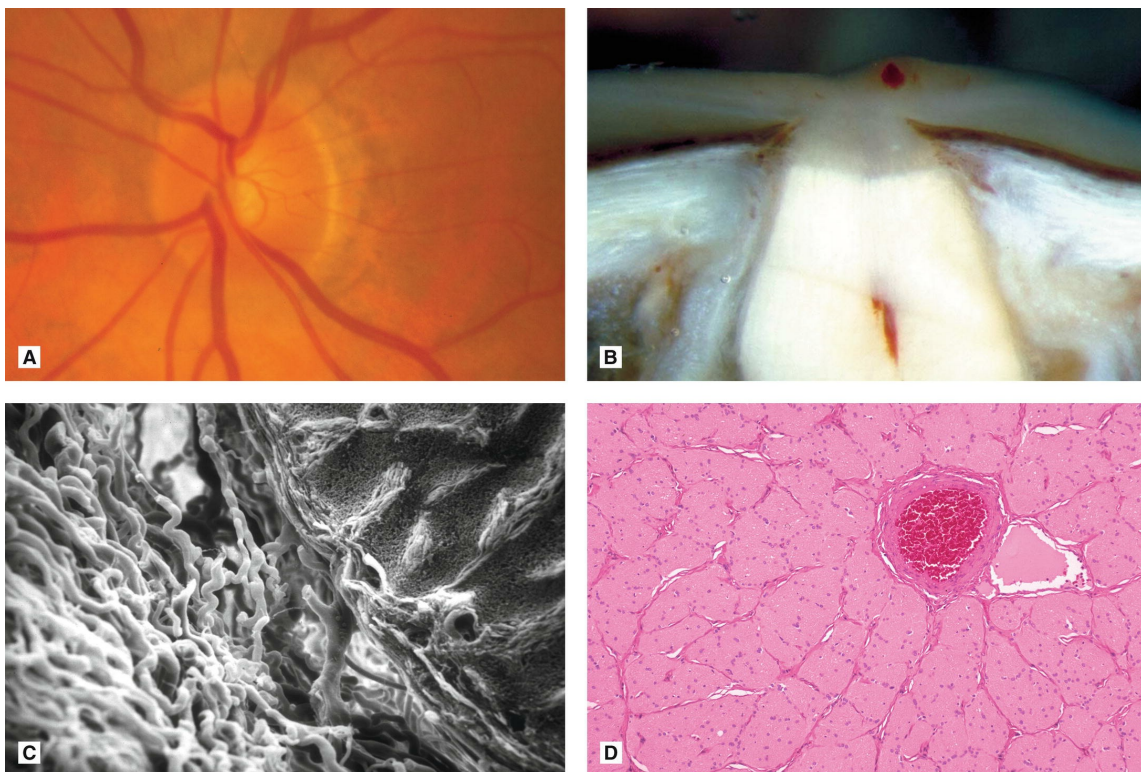


FIG. 1-10. The optic nerve. **A.** The optic disk is ~1.5 mm in vertical diameter. **B.** Longitudinally sectioned optic nerve shows abrupt termination of creamy myelin at the posterior margin of the lamina cribrosa. **C.** SEM of optic nerve meninges shows spidery arachnoidal processes bridging cleft between the optic nerve (**at right**) and the dura (**at left**). Septa of pia mater extend into the substance of the nerve, compartmentalizing its axons. **D.** Pial septa and central retinal vessels are seen in photomicrograph of transversely sectioned nerve. (**C.** SEM $\times 160$, **D.** H&E $\times 100$.)

BIBLIOGRAPHY

-
- Fine BS, Yanoff M. *Ocular Histology: A Text and Atlas*, 2nd ed. Hagerstown, MD: Harper & Row, 1979.
- Hogan MJ, Alvarado JA, Weddell JE. *Histology of the Human Eye*. Philadelphia, PA: W.B. Saunders, 1971.
- Jakobiec FA. *Ocular Anatomy, Embryology, and Teratology*. Philadelphia, PA: Harper & Row, 1982.
- Snell RS, Lemp MA. *Clinical Anatomy of the Eye*, 2nd ed. Boston, MA: Blackwell Scientific Publications, 1998.
- Wobmann PR, Fine BS. The clump cells of Koganei. A light and electronmicroscopic study. *Am J Ophthalmol* 1972;73(1):90–101.